

Temperature dependence and deuterium kinetic isotope effects in the HCO + NO reaction

John D. DeSain¹, Leonard E. Jusinski, Craig A. Taatjes*

Combustion Research Facility, Mail Stop 9055, Sandia National Laboratories,
Livermore, CA 94551-0969, USA

Received 12 July 2005; received in revised form 28 July 2005; accepted 28 July 2005

Available online 30 August 2005

Abstract

The reactions of HCO and DCO with NO have been measured by the laser photolysis/continuous-wave (CW) laser-induced fluorescence (LIF) method from 296 to 623 K, probing the ($\tilde{B}^2A' \leftarrow \tilde{X}^2A'$) HCO (DCO) system. The HCO+NO rate coefficient is $(1.81 \pm 0.10) \times 10^{-11} \text{ cm}^3 \text{ molecule}^{-1} \text{ s}^{-1}$ and the DCO+NO rate coefficient is $(1.61 \pm 0.12) \times 10^{-11} \text{ cm}^3 \text{ molecule}^{-1} \text{ s}^{-1}$ at 296 K. Both rate coefficients decrease with increasing temperature between 296 and 623 K. The kinetic isotope effect is $k_H/k_D = 1.12 \pm 0.09$ at 296 K and increases to 1.25 ± 0.15 at 623 K. The normal kinetic isotope effect supports abstraction as the principal mechanism for the reaction, in agreement with recent computational results.

© 2005 Elsevier B.V. All rights reserved.

Keywords: Chemical kinetics; HCO; Combustion chemistry

1. Introduction

Reactions of the formyl radical (HCO) are key processes in atmospheric chemistry and combustion. The reaction of HCO with nitric oxide (NO) is important in systems such as the combustion of chemical explosives [1] and solid propellants [2,3], and for formaldehyde production in lean-burn natural gas engines [4]. The kinetics of this reaction have been studied near room temperature by several groups, but only one temperature-dependent measurement of the rate coefficient has been performed. The room-temperature measurements before 2000 are in relatively good agreement [5–9], with rate coefficients between 1.2×10^{-11} and $1.45 \times 10^{-11} \text{ cm}^3 \text{ molecule}^{-1} \text{ s}^{-1}$. The measurements of Veyret and Lesclaux [9] showed a slight negative tem-

perature dependence between 298 and 503 K, with a rate coefficient of $(1.23 \pm 0.12) \times 10^{-11} \text{ cm}^3 \text{ molecule}^{-1} \text{ s}^{-1}$ at 298 K. However, Veyret and Lesclaux [9] suggested that the reliability of their HCO+NO rate coefficients could be poorer than indicated by the estimated error, and criticized the methodology of several earlier measurements. Cavity ring-down measurements by Ninomiya et al. [10] in 2000 yielded a rate coefficient of $(1.9 \pm 0.2) \times 10^{-11} \text{ cm}^3 \text{ molecule}^{-1} \text{ s}^{-1}$ at 295 K, and relative-rate measurements reported in the same work yielded a rate coefficient of $(2.1 \pm 0.5) \times 10^{-11} \text{ cm}^3 \text{ molecule}^{-1} \text{ s}^{-1}$. The similar reaction of HCO+O₂ showed a comparable discrepancy [10], and more recent measurements using laser-induced fluorescence [11,12] and diode laser absorption [13] have tended to corroborate the results of Ninomiya et al. for HCO+O₂. A reinvestigation of the temperature-dependent kinetics of the HCO+NO reaction therefore appears warranted.

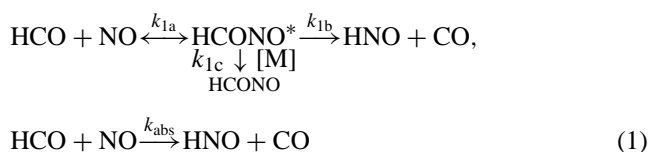
Furthermore, the mechanism of the HCO+NO reaction has been open to question. It can proceed via a covalently bound complex (HC(O)NO) with subsequent formation of

* Corresponding author. Tel.: +1 925 294 2764.

E-mail address: cataatj@sandia.gov (C.A. Taatjes).

¹ Present address: The Aerospace Corporation, 2350 E. El Segundo Blvd., El Segundo, CA 90245-4691, USA.

products (HNO and CO) or by direct hydrogen abstraction:



Historically, the experimental evidence has appeared to favor the participation of the bound intermediate in the reaction. Observation of stabilized HCONO formed from the HCO+NO reaction in the gas phase has been reported by Napier and Norrish [14]. Langford and Moore measured kinetic isotope effects [8] and removal of vibrationally excited HCO by NO [15] and concluded that complex formation followed by elimination (k_{1a} and k_{1b}) dominated the reaction. Butkovskaya et al. [16,17] observed population in the excited states of ν_1 and ν_2 of HNO from the HCO+NO reaction at 298 K, and described their results as consistent with formation via a long lived complex rather than by direct hydrogen abstraction. Ab initio statistical predictions by Kulkarni and Koga [18] suggest that the hydrogen abstraction channel for HCO+NO is too slow to contribute significantly to the total reaction rate at 298 K (with an estimated rate coefficient of $\sim 1 \times 10^{-17} \text{ cm}^3 \text{ s}^{-1}$).

However, Xu et al. [19] have very recently carried out a detailed high-level characterization of stationary points on the HCO+NO potential energy surfaces and have determined that the direct abstraction has no barriers above the energy of the entrance channel. In addition, master equation calculations using the ab initio stationary points showed excellent agreement with literature rate coefficients and predicted a dominant direct abstraction mechanism [19].

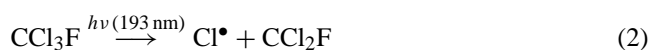
The only previous measurement of the kinetic isotope effect for HCO+NO is that of Langford and Moore [8]. They observed that deuterium substitution increases the rate coefficient, with ($k_{\text{H}}/k_{\text{D}} = 0.81 \pm 0.14$) for HCO+NO and ($k_{\text{H}}/k_{\text{D}} = 0.91 \pm 0.17$) for HCO+O₂. The inverse kinetic isotope effect in both reactions was taken as evidence for the participation of a long-lived complex. However, subsequent experiments on the HCO+O₂ system [11] observed no significant kinetic isotope effect for deuteration of the HCO ($k_{\text{H}}/k_{\text{D}} = 1.00 \pm 0.07$). An abstraction reaction, as predicted by the most recent theoretical investigation of the HCO+NO reaction [19], is usually associated with normal kinetic isotope effects. The uncertainty estimates of the Langford and Moore [8] HCO+NO measurements do not encompass the possibility of a normal isotope effect, and appear difficult to reconcile with a direct abstraction mechanism. The present work re-examines this kinetic isotope effect.

This study measures the HCO+NO and DCO+NO reaction rate coefficients as a function of temperature (296–623 K). The time behavior of the HCO radical is observed directly by using a laser photolysis/CW laser-induced fluorescence (cwLIF) method. The ($\tilde{B}^2A' \leftarrow \tilde{X}^2A'$) system of both isotopomers has been previously characterized [20–22] and provides an excellent means of observing

the progress of the reaction for either isotopomer independently. Because of the relatively small concentration of HCO, and hence photolytic precursor, needed for LIF detection, the contributions of side reactions such as HCO self-reaction or reactions with the photolysis precursor are limited. The Cl abstraction from formaldehyde is chosen for reaction initiation because it reduces the possibility of side reaction with counter species such as H, CH₃, and CH₃CO produced from acetaldehyde or formaldehyde photolysis. The rate coefficient measured at room temperature (296 K) is $(1.81 \pm 0.12) \times 10^{-11} \text{ cm}^3 \text{ molecule}^{-1} \text{ s}^{-1}$, in good agreement with the recent results of Ninomiya et al. [10]. The rate coefficients decrease with increasing temperature as previously observed by Veyret and Lesclaux [9]. A small but significant normal kinetic isotope effect is observed, contrary to the previous kinetic isotope effect measurements of Langford and Moore [8].

2. Experiment

The reaction of HCO (DCO)+NO is investigated by using the laser photolysis/CW laser-induced fluorescence (LP/cwLIF) method, similar to that employed in previous experiments [11,23]. The experiments are performed in a slow-flow reactor, where the gas flow (about 30 cm s⁻¹) is slow compared to the reaction time scale, but fast enough to fully replenish the approximately 0.5 cm high reaction zone between photolysis pulses (at repetition rates between 2 and 10 Hz). The reaction is initiated by Cl abstraction from formaldehyde (H₂CO). The Cl is generated by photolysis of CCl₃F at 193 nm, and the HCO or DCO radical is produced by subsequent Cl reaction with H₂CO or D₂CO. In some cases the reaction is initiated by direct photolysis of formaldehyde. The HCO (DCO) then reacts with NO:



The progress of the HCO (DCO)+NO reaction is monitored by LIF in the ($\tilde{B}^2A' \leftarrow \tilde{X}^2A'$) system using the output of a continuous-wave ring dye laser operating near 516 nm [11,24]. The ring laser output is doubled in an external buildup cavity that uses a BBO crystal as the second harmonic generation medium. The doubled probe beam ($\leq 50 \text{ mW cm}^{-2}$) at 38692.6 cm^{-1} (38631.6 cm^{-1} for DCO experiments) enters the flow reactor through a CaF₂ window. The unfocused photolysis beam (3 mJ/pulse) first passes through an aperture and then enters the reactor through a different window at a right angle to the probe beam. The fluorescence is detected perpendicular to both laser beams with a photomultiplier tube operating in single photon counting mode. A filter is placed between the photomultiplier tube and the reactor to remove stray 193 nm light. The photomul-

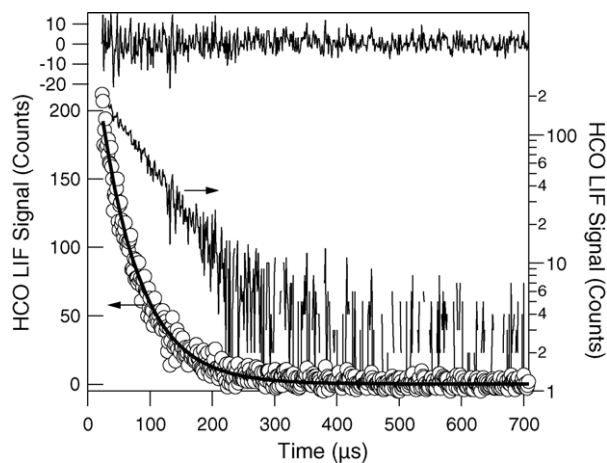


Fig. 1. The time profile of the cwLIF signal for HCO taken at 296 K and 10.0 Torr with $6.49 \times 10^{14} \text{ cm}^{-3}$ of NO. The HCO signal (open circles) is fit by an exponential, with the residuals shown above. The signal is also shown as a solid line on a logarithmic scale given on the right, demonstrating single-exponential decay. The time constant of the decay corresponds to a pseudo-first order rate coefficient of $14,200 \text{ s}^{-1}$.

tiplier output is transferred to a multichannel scaler, where typically 2048 channels with a width of $1.28 \mu\text{s}$ are accumulated. To remove the influences of stray photolysis light a chopper wheel is used to allow subtraction of the signal with the probe beam blocked. To achieve a good signal-to-noise ratio the signal is typically added over 12,000 excimer laser shots.

The stainless steel flow reactor is resistively heated. The temperature of the cell is monitored by a retractable thermocouple placed inside the cell directly over the reaction zone. The gas flows are controlled by calibrated mass flow meters, and the pressure in the reactor is monitored with a capacitance manometer. Typical gas concentrations are $[\text{NO}] = 0.2 \times 10^{15} \text{ cm}^{-3}$ to $1.5 \times 10^{15} \text{ cm}^{-3}$, $[\text{CCl}_3\text{F}] = 6 \times 10^{15}$, and $[\text{H}_2\text{CO}] = 3 \times 10^{15} \text{ cm}^{-3}$. Helium is added to a total density of $3.25 \times 10^{17} \text{ cm}^{-3}$. The initial HCO concentrations are estimated to be $\sim 10^{13} \text{ cm}^{-3}$. Both initiation reactions could produce vibrationally excited HCO. The relaxation into the probed state will contribute to the observed rise of the signal, and the timescale of this vibrational energy transfer is empirically determined from LIF measurements in the absence of NO [11]. Under the present conditions vibrational relaxation of both isotopomers is complete before the kinetics of the reaction of interest are measured. The reactions are monitored under pseudo-first order conditions, where $[\text{NO}] \gg [\text{HCO}]$. The HCO time profile can then be fitted by a single exponential, and the second order rate coefficient is obtained from the slope of a plot of the pseudo-first order rate coefficient versus $[\text{NO}]$.

3. Results and discussion

Fig. 1 shows the time-resolved HCO LIF signal created by $\text{Cl} + \text{H}_2\text{CO}$ in the presence of $6.49 \times 10^{14} \text{ cm}^{-3}$ of

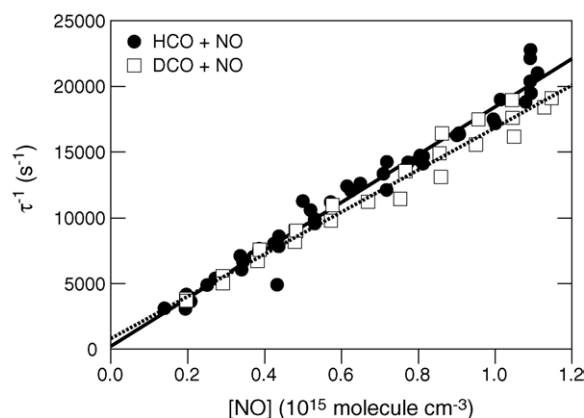


Fig. 2. Pseudo-first order rate coefficient as a function of NO concentration at 296 K and 10 Torr for HCO+NO (solid circles) and DCO+NO (open squares). The linear fits yield a second order rate coefficients $k_{\text{H}} = (1.81 \pm 0.10) \times 10^{-11} \text{ cm}^3 \text{ molecule}^{-1} \text{ s}^{-1}$ (solid line) and $k_{\text{D}} = (1.61 \pm 0.12) \times 10^{-11} \text{ cm}^3 \text{ molecule}^{-1} \text{ s}^{-1}$ (dotted line).

Table 1

Measured second order rate coefficients for HCO (DCO)+NO at different temperatures

Reaction	HCO source	Temperature (K)	k ($\text{cm}^3 \text{ molecule}^{-1} \text{ s}^{-1}$)
HCO+NO	Cl abstraction	296	$(1.81 \pm 0.10) \times 10^{-11}$
HCO+NO	Cl abstraction	323	$(1.79 \pm 0.08) \times 10^{-11}$
HCO+NO	Cl abstraction	373	$(1.55 \pm 0.09) \times 10^{-11}$
HCO+NO	Cl abstraction	423	$(1.31 \pm 0.08) \times 10^{-11}$
HCO+NO	Cl abstraction	473	$(1.19 \pm 0.09) \times 10^{-11}$
HCO+NO	Cl abstraction	523	$(1.12 \pm 0.11) \times 10^{-11}$
HCO+NO	Cl abstraction	573	$(1.09 \pm 0.08) \times 10^{-11}$
HCO+NO	Cl abstraction	623	$(1.07 \pm 0.08) \times 10^{-11}$
DCO+NO	Cl abstraction	296	$(1.61 \pm 0.12) \times 10^{-11}$
DCO+NO	Cl abstraction	473	$(0.96 \pm 0.08) \times 10^{-11}$
DCO+NO	Cl abstraction	573	$(0.87 \pm 0.09) \times 10^{-11}$
DCO+NO	D ₂ CO photolysis	296	$(1.60 \pm 0.10) \times 10^{-11}$
HCO+NO	H ₂ CO photolysis	296	$(1.82 \pm 0.11) \times 10^{-11}$

NO at 296 K and 10 Torr of total pressure. The residuals show that the decay of the HCO is described well by a single exponential. A plot of the inverse of the exponential time constant τ (i.e., the pseudo-first order rate coefficient) against $[\text{NO}]$ is shown in Fig. 2 for HCO+NO at 296 K and 10 Torr total pressure. The linear fit in Fig. 2 yields a second order rate coefficient of $(1.81 \pm 0.10) (2\sigma) \times 10^{-11} \text{ cm}^3 \text{ molecule}^{-1} \text{ s}^{-1}$. The rate coefficient at 296 K obtained by using photolysis of formaldehyde as the HCO source is $(1.82 \pm 0.12) \times 10^{-11} \text{ cm}^3 \text{ molecule}^{-1} \text{ s}^{-1}$, as listed in Table 1. No difference is observed when using either Cl abstraction or formaldehyde photolysis to generate HCO or DCO.

The second order rate coefficients for both HCO + NO and DCO + NO obtained at different temperatures are listed in Table 1. All the experiments are carried out at a total density of $3.25 \times 10^{17} \text{ cm}^{-3}$. The second order rate coefficient versus temperature is shown in Fig. 3 for temperatures between 296 K and 623 K. The temperature dependence of the second order rate coefficient for HCO + NO is well-represented by

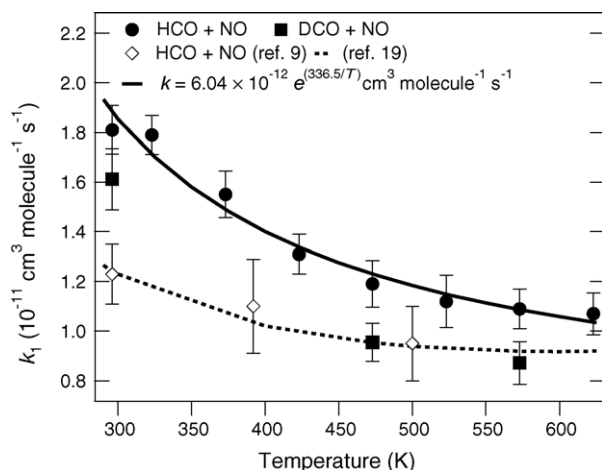


Fig. 3. The temperature dependence of the second order rate coefficient for HCO + NO (●) and DCO + NO (■) measured at a constant density of $3.25 \times 10^{17} \text{ cm}^{-3}$. Error bars represent $\pm 2\sigma$ precision. The solid line shows the fit of the second order rate coefficient to a simple Arrhenius expression, $k_1 = 6.04 \times 10^{-12} e^{336.5/T} \text{ cm}^3 \text{ molecule}^{-1} \text{ s}^{-1}$. The temperature dependent second order rate coefficients for HCO + NO from Veyret and Lesclaux [9] (◇) and the calculations of Xu et al. [19] (dotted line) are also shown for comparison.

$k_1 = 6.04 \times 10^{-12} e^{336.5/T} \text{ cm}^3 \text{ molecule}^{-1} \text{ s}^{-1}$. Fig. 3 shows that the DCO + NO rate coefficient decreases with increased temperature between 296 K and 573 K as well. Veyret and Lesclaux [9] also measured a decrease of the rate coefficient with increasing temperature, but the current rate coefficient measurements show a slightly steeper decline of the rate coefficient with increasing temperature. The current measurements also give a somewhat larger rate coefficient at each temperature than those measured by Veyret and Lesclaux or the calculations of Xu et al. [19].

The six previous measurements [5–10] of the HCO + NO rate coefficient at room temperature are listed in Table 2. Many techniques have been used to measure this reaction, including intra-cavity dye laser spectroscopy (IDLS) [5,6], laser resonance absorption (LRA) [8,9], photoionization mass spectrometry (PIMS) [7], and cavity ring-down spectroscopy (CRDS) [10]. Five of the measurements yield fairly consistent values for the HCO + NO rate coefficient despite differences in the method used. However, there is

evidence that this harmony may be misleading. These previous six experiments all also observed the rate coefficient of the reaction of HCO + O₂. The results of Veyret and Lesclaux [9] and Ninomiya et al. [10] for HCO + O₂ agree with most recent measurements [11–13,25] of the HCO + O₂ rate coefficient. There is a general agreement among these recent experiments for a higher HCO + O₂ rate coefficient than observed in the other four experiments listed in Table 2 ($\sim 5.6 \times 10^{-12} \text{ cm}^3 \text{ s}^{-1}$ rather than $\sim 4.2 \times 10^{-12} \text{ cm}^3 \text{ s}^{-1}$). The Ninomiya et al. [10] study also found that the HCO + NO rate coefficient was significantly larger than the other five previous measurements listed in Table 2. They suggest that not only was the HCO + O₂ rate coefficient underestimated in previous studies but that the HCO + NO rate coefficient may also have been underestimated.

The rate coefficient at room temperature obtained in this work is in good agreement with the measurement of Ninomiya et al. [10]. This result is $\sim 40\%$ larger than the other experiments listed in Table 2. The Langford and Moore [8] results should not suffer from the reactant depletion effects of the IDLS measurements, discussed by Veyret and Lesclaux [9]. Nevertheless the Langford and Moore HCO + O₂ rate coefficient and HCO + NO rate coefficient are lower than the Ninomiya et al. [10] measurements and the current results. The two experiments also used different experimental techniques (CRDS in the Ninomiya et al. measurements, LRA in the Langford and Moore work), but it is unclear why the results differ. The Ninomiya et al. [10] and the Langford and Moore [8] experiments monitored the HCO radicals using the same transition $\tilde{A}^2A''(090) \leftarrow \tilde{X}^2A'(000)$, although Ninomiya et al. used the R branch whereas Langford and Moore used the Q branch. The CRDS measurements were able to work with smaller HCO concentrations. The CRDS determinations of Ninomiya et al. are in agreement with the relative rate study in the same paper that measured the HCO + NO, HCO + O₂ and HCO + NO₂ rate coefficients relative to the HCO + Cl₂ reaction rate coefficient [10]. Furthermore, the derived rate coefficient for HCO + NO₂ ($6.3 \pm 1.5 \times 10^{-11} \text{ cm}^3 \text{ molecule}^{-1} \text{ s}^{-1}$), is in agreement with a recent measurement of Guo et al. [26] ($(5.7 \pm 0.9) \times 10^{-11} \text{ cm}^3 \text{ molecule}^{-1} \text{ s}^{-1}$), performed with the same technique as the Langford and Moore experiments [8]. While the source of the discrepancy in rate coefficient

Table 2
Observed rate coefficients for HCO + NO and HCO + O₂ at room temperature

$k_{\text{HCO}+\text{NO}}$ ($10^{-11} \text{ cm}^3 \text{ molecule}^{-1} \text{ s}^{-1}$)	$k_{\text{HCO}+\text{O}_2}$ ($10^{-12} \text{ cm}^3 \text{ molecule}^{-1} \text{ s}^{-1}$)	Method	Reference
1.2 ± 0.4	3.8 ± 1.0	Flash photolysis/intracavity laser spectroscopy	[5]
1.4 ± 0.2	4.0 ± 0.7	Flash photolysis/intracavity laser spectroscopy	[6]
1.3 ± 0.2	4.0 ± 0.6	Discharge flow/photoionization mass spectrometry	[7]
1.3 ± 0.2	4.6 ± 0.6	Laser photolysis/laser absorption	[8]
1.2 ± 0.2	5.6 ± 0.6	Laser photolysis/laser absorption	[9]
1.9 ± 0.2	5.9 ± 0.5	Laser photolysis/cavity ring-down spectroscopy	[10]
–	5.6 ± 0.3	Laser photolysis/laser-induced fluorescence	[11]
1.8 ± 0.1	–	Laser photolysis/laser-induced fluorescence	This work

measurements remains uncertain, as discussed by Ninomiya et al. [10], the present results support the higher value for the rate coefficient.

The kinetic isotope effect is represented by the ratio of the second order rate coefficients ($k_{\text{H}}/k_{\text{D}}$). The HCO+NO reaction displays a normal isotope effect, with the HCO+NO reaction $\sim 12\%$ faster than the reaction of DCO+NO at room temperature. At higher temperature the isotope effect appears to increase, with $k_{\text{H}}/k_{\text{D}} = 1.12 \pm 0.09$ at 296 K, $k_{\text{H}}/k_{\text{D}} = 1.25 \pm 0.14$ at 473 K and $k_{\text{H}}/k_{\text{D}} = 1.25 \pm 0.15$ at 573 K. This result is in qualitative disagreement with the determination of $k_{\text{H}}/k_{\text{D}} = 0.81 \pm 0.14$ by Langford and Moore [8]. Interestingly, the Langford and Moore measurement of the DCO+NO rate coefficient at room temperature ($(1.56 \pm 0.2) \times 10^{-11} \text{ cm}^3 \text{ molecule}^{-1} \text{ s}^{-1}$) is in good agreement with the present results. The previously reported DCO+O₂ rate coefficient from this laboratory [11] ($(5.61 \pm 0.23) \times 10^{-12} \text{ cm}^3 \text{ molecule}^{-1} \text{ s}^{-1}$) is encompassed within the DCO+O₂ rate coefficient error estimates of Langford and Moore ($(5.1 \pm 0.7) \times 10^{-12} \text{ cm}^3 \text{ molecule}^{-1} \text{ s}^{-1}$) [8]. It is unclear why the absorption experiments of Langford and Moore should underestimate the rate coefficients for the HCO+O₂ and HCO+NO reactions. However if the HCO+O₂ and NO rate coefficients (but not the DCO+O₂ and NO rate coefficients) were underestimated in the Langford and Moore experiment it would explain the different kinetic isotope effect from the present experiments.

The kinetic isotope effect in a complex-mediated reaction can reflect a balance among the isotope effects for stabilization, redissociation to reactants and formation of products. The inverse kinetic isotope effects observed by Langford and Moore were explained by a model for the HCO+NO and HCO+O₂ reactions that included significant redissociation of the complex to reactants. Given the normal kinetic isotope effect measured in the present study, the returning flux from the HC(O)NO complex need not be large. This interpretation is supported by the rate coefficients for the complex at 298 K predicted by Kulkarni and Koga [18] using RRKM (Rice–Ramsperger–Kassel–Marcus) theory. The redissociation of HC(O)NO to the reactants is predicted to be $4.0 \times 10^{-4} \text{ s}^{-1}$ at 298 K. However, Kulkarni and Koga were unable to find a product pathway with a lower energy barrier than the reactant channel, and concluded that another reaction pathway must exist that was not found in their ab initio calculations [18].

Recently, Xu et al. [19] addressed the mechanism of the HCO+NO reaction using master equation calculations and variational transition-state theory, based on new high-level calculations of stationary points on both the triplet and singlet surfaces. They established that the abstraction pathway has no barriers above reactants and should dominate the reaction. In subsequent unpublished work, Xu and Lin [27] have calculated the DCO+NO rate coefficient (and hence the kinetic isotope effect) by the same method. The calculated kinetic isotope effect decreases from 1.36 at 200 K to

1.21 at 800 K. The room temperature kinetic isotope effect of 1.12 ± 0.09 measured in this work is significantly smaller than the calculated effect of 1.34 [27], but the measurements at 473 and 573 K are in excellent agreement with the calculated values of 1.29 (473 K) and 1.26 (573 K) [27]. Hydrogen atom abstraction reactions typically display normal deuterium kinetic isotope effects, reflecting in part the difference in zero-point energies between reactants and the transition state. The rate coefficient for the abstraction channel in the HCO+NO reaction is affected by the presence of a hydrogen-bonded complex in the entrance channel. The transition state to abstraction via the hydrogen-bonded well lies approximately 1 kcal mol^{-1} below the reactants, but reflection from this transition state changes the calculated rate coefficient by a factor of 2.57 at room temperature [19]. The kinetic isotope effect may be modified by the effects of the hydrogen-bonded complex. For comparison, the calculated kinetic isotope effect for the HCO+O₂ reaction, which is mediated by the covalently bonded HC(O)O₂ well, is $\sim 1.15\text{--}1.20$ [28]. The present results appear consistent with the newest calculations, suggesting that abstraction, mediated by a weakly bound complex, is the principal mechanism for the HCO+NO reaction.

4. Conclusions

The HCO+NO and DCO+NO reactions have been investigated as a function of pressure and temperature. The room temperature rate coefficients are $k_{\text{HCO+NO}} = (1.81 \pm 0.10) \times 10^{-11} \text{ cm}^3 \text{ molecule}^{-1} \text{ s}^{-1}$ and $k_{\text{DCO+NO}} = 1.61 \pm 0.12 \times 10^{-11} \text{ cm}^3 \text{ molecule}^{-1} \text{ s}^{-1}$. The rate coefficients decrease when the temperature is increased from 296 K to 623 K. A small normal kinetic isotope effect is observed ($k_{\text{H}}/k_{\text{D}} = 1.12 \pm 0.09$ at 296 K). The observed rate coefficient at 296 K is larger than most previous determinations, but in agreement with the most recent measurement, suggesting an upward revision of the rate coefficient. The kinetic isotope effect is in disagreement with the previous observation, but appears consistent with the highest-level calculations of the HCO+NO reaction that suggest a direct abstraction mechanism.

Acknowledgements

Dr. Z.F. Xu and Prof. M.C. Lin are gratefully acknowledged for performing calculations of the DCO+NO rate coefficients and kinetic isotope effects and for generously sharing their results. This work is supported by the Division of Chemical Sciences, Geosciences, and Biosciences, the Office of Basic Energy Sciences, the U.S. Department of Energy. Sandia is a multi-program laboratory operated by Sandia Corporation, a Lockheed Martin Company, for the National Nuclear Security Administration under contract DE-AC04-94-AL85000.

References

- [1] R. Guirguis, D. Hsu, D. Bogan, E. Oran, *Combust. Flame* 61 (1985) 51.
- [2] M.H. Alexander, P.J. Dagdigian, M.E. Jacox, C.E. Kolb, C.F. Melius, H. Rabitz, M.D. Smooke, W. Tsang, *Prog. Energy Combust. Sci.* 17 (1991) 263.
- [3] G.F. Adams, R.W. Shaw Jr., *Annu. Rev. Phys. Chem.* 43 (1992) 311.
- [4] P. Glarborg, M.U. Alzueta, K. Kjærsgaard, K. Dam-Johansen, *Combust. Flame* 132 (2003) 629.
- [5] V.A. Nadochenko, O.M. Sarkisov, V.I. Vedeneev, *Dokl. Phys. Chem.* 244 (1979) 152.
- [6] J.H. Clark, C.B. Moore, J.P. Reilly, *Int. J. Chem. Kinet.* 10 (1978) 427.
- [7] F.L. Nesbitt, J.F. Gleason, L.J. Stief, *J. Phys. Chem. A* 103 (1999) 3038.
- [8] A.O. Langford, C.B. Moore, *J. Chem. Phys.* 80 (1984) 4211.
- [9] B. Veyret, R. Lesclaux, *J. Phys. Chem.* 85 (1981) 1918.
- [10] Y. Ninomiya, M. Goto, S. Hashimoto, Y. Kagawa, K. Yoshizawa, M. Kawasaki, T.J. Wallington, M.D. Hurley, *J. Phys. Chem. A* 104 (2000) 7556.
- [11] J.D. DeSain, L.E. Jusinski, A.D. Ho, C.A. Taatjes, *Chem. Phys. Lett.* 347 (2001) 79.
- [12] K. Yamasaki, M. Sato, A. Itakura, A. Watanabe, T. Kakuda, I. Tokue, *J. Phys. Chem. A* 104 (2000) 6517.
- [13] B. Hanoune, S. Dusanter, L. ElMaimouni, P. Devolder, B. Lemoine, *Chem. Phys. Lett.* 343 (2001) 527.
- [14] I.M. Napier, F.R.S. Norrish, *Proc. R. Soc. Lond. Ser. A* 299 (1967) 337.
- [15] A.O. Langford, C.B. Moore, *J. Chem. Phys.* 80 (1984) 4204.
- [16] N.I. Butkovskaya, D.W. Setser, *J. Phys. Chem. A* 102 (1998) 9715.
- [17] N.I. Butkovskaya, A.A. Muravyov, D.W. Setser, *Chem. Phys. Lett.* 266 (1997) 223.
- [18] S.A. Kulkarni, N. Koga, *J. Phys. Chem. A* 102 (1998) 5228.
- [19] Z.F. Xu, C.-H. Hsu, M.C. Lin, *J. Chem. Phys.* 122 (2005) 234308.
- [20] G.W. Adamson, X.S. Zhao, R.W. Field, *J. Mol. Spectrosc.* 160 (1993) 11.
- [21] Y.J. Shiu, I.-C. Chen, *J. Mol. Spectrosc.* 165 (1994) 457.
- [22] J. Gripp, A. Kuczmann, C. Stöck, F. Temps, A. Tröllsch, *Phys. Chem. Chem. Phys.* 2 (2000) 1653.
- [23] H. Thiesemann, E.P. Clifford, C.A. Taatjes, S.J. Klippenstein, *J. Phys. Chem. A* 105 (2001) 5393.
- [24] L.E. Jusinski, C.A. Taatjes, *Rev. Sci. Instrum.* 72 (2001) 2837.
- [25] R.S. Timonen, E. Ratajczak, D. Gutman, *J. Phys. Chem.* 92 (1988) 651.
- [26] Y. Guo, S.C. Smith, C.B. Moore, C.F. Melius, *J. Phys. Chem.* 99 (1995) 7473.
- [27] Z.F. Xu, M.C. Lin, Personal Communication, 2005.
- [28] C.C. Hsu, A.M. Mebel, M.C. Lin, *J. Chem. Phys.* 105 (1996) 2346.